Current Journal of Applied Science and Technology

Volume 43, Issue 1, Page 35-45, 2024; Article no.CJAST.111693
ISSN: 2457-1024
(Past name: British Journal of Applied Science & Technology, Past ISSN: 2231-0843, NLM ID: 101664541)

Contribution to the Study of the Breaking Behavior of Starch-Based Composite Films: Numerical and Mathematical Analysis of the Effects of Reinforcement and Temperature

Doumbia Ahmed [a*] and Traoré Seydou [b]

[a] Faculty of Environment, Jean Lorougnon Guédé University, Ivory Coast.
[b] Faculty of Structural Sciences, Materials and Technologies, Félix Houphouët-Boigny University, Ivory Coast.

Authors' contributions

This work was carried out in collaboration between both authors. Both authors read and approved the final manuscript.

Article Information

DOI: 10.9734/CJAST/2024/v43i24347

Open Peer Review History:
This journal follows the Advanced Open Peer Review policy. Identity of the Reviewers, Editor(s) and additional Reviewers, peer review comments, different versions of the manuscript, comments of the editors, etc are available here: https://www.sdiarticle5.com/review-history/111693

Original Research Article

Received: 15/11/2023
Accepted: 20/01/2024
Published: 23/01/2024

ABSTRACT

Our previous article focused on the analysis of crack propagation in a composite film based on cassava starch reinforced with coconut fibers. The price parameters taken into account in this study are the size and position of the crack, and the applied load. The aim of this work is to analyze the breaking behavior of said material. To do this, the effects of variations in temperature and fibers, key factors influencing the thermomechanical behavior of the film, will be illustrated. We will adopt an approach based on the displacement of the crack tip using the extended finite element method (XFEM). A calculation by numerical simulation using the Cast3M finite element calculation code will

**Corresponding author: E-mail: fackoly1@gmail.com;*

be carried out based on an established behavioral law. This phase will be followed by a mathematical study in order to establish a homogenized analytical model representative of the breaking behavior of the composite. The results obtained in the two cases are very consistent. The reinforcements increase the resistance to rupture while a rise in temperature promotes deterioration of the material. They make it possible to describe and predict the breaking behavior of the composite films subject to this study.

Keywords: Starch; film; rupture; reinforcements; temperature.

ABBREVIATIONS

L : Half Length of Crack (mm)
W : Length of Specimen (mm)
E_i *: Young's modulus of the phase i (MPa)*
E_{oi} *:Young's Modulus of the Phase i at the Initial Temperature T = 0 °C*
R_{ei} *: elastic limit of the phase i (MPa)*
C_s *: safety coeficient;*
α_{thi} *: Coefficient of Thermal Expansion of the Phase i (°C^{-1})*
ΔT *: Temperature Variation (°C)*
n : Number of Inclusion Subfamilies
f^i *: Volume Fraction*
C^i *: Average Stiffness Tensor*
A^i *: Strain Localization Tensor*
V : Sample Volume (m^3)
dv : Elementary Volume of the Sample (m^3)
ε_{ij} *: Components of Deformations in dv*
C_{ijkl} *: Component of the Stiffness Tensor (MPa)*
$\sum_{ij}$ *: Composite stress Tensor Component (MPa)*
V^r, V^m : Respective Volumes of the Reinforcement and the Matrix
u, v : Respectively Horizontal and Vertical Displacements of the Crack Tip
k : Kolosov Constant in Plane Strains
v *: Poison Coefficient of the Material*
μ *: Lamé Coefficient*
K_I, K_{II} : Stress Intensity Factors (FIC) in Mode 1 and 2 Respectively

1. INTRODUCTION

The behavior of a composite material depends, in part, on the volume fractions of the different constituents. This was illustrated in our previous work [1, 2] for the film subject of this article. In this work, it was shown that variations in temperature and volume fraction of the fibers have a very considerable impact on the mechanical behavior. Our work aims to analyze the effects of these two factors, temperature and reinforcement, on the fracture behavior of the present composite, the subject of our study. We will adopt the crack tip displacement approach by applying the extended finite element method (XFEM). Indeed, from a law of thermomechanical behavior established in one of our articles [2], we will establish a model of homogenized thermomechanical behavior inspired by Voigt's hypothesis. This step will be followed by a calculation by numerical simulation using the Cast3M finite element calculation code. Finally, the homogenized moving crack propagation model based on the analytical solutions of Westergaard [3] will be established. Comparison of the results of the two methods are very consistent.

2. GENERAL HYPOTHESES

In this study we make the following general hypotheses:

- The composite film is elasto-damageable and isotropic.
- The composite film is homogeneous or at least homogeneous in pieces.
- The composite only undergoes plane deformations.

- The crack is centered on the film with an angle of inclination relative to the direction orthogonal to that of the stress.
- The dimensions of the film are assumed to be infinite compared to the size of the crack.

The Fig 1 gives the geometric representation of the cracked film under loading.

3. HOMOGENIZED THERMOMECHANICAL BEHAVIOR LAW

For a homogeneous and isotropic material, from Hooke's law and taking into account the initial conditions of zero deformation, we show that the rigidity is expressed as follows [2, 4]:

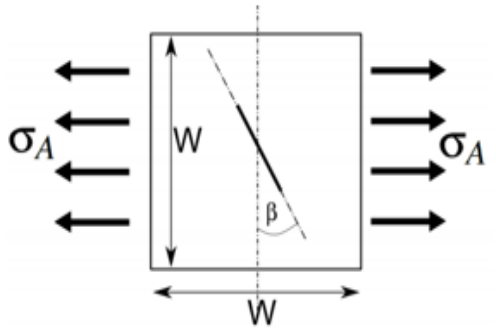

Fig. 1. Film under tensile stress with centered and inclined crack

$$E_i = \frac{E_{oi}}{R_{ei}}(R_{ei} - C_s E_{oi}\alpha_{thi}\Delta T) \quad (1)$$

with : i = r (reinforcement) or m (matrix) ;

On the other hand, the homogenized stiffness of the composite is given by [5] :

$$E = \sum_0^n f^i C^i A^i \quad (2)$$

Voigt assumes that the deformation in each phase is identical to the applied macroscopic deformation, therefore homogeneous [6]. In this context, if we subject the film to a component deformation E_{ij}, we have :

$$E_{ij} = \frac{1}{V}\iiint \varepsilon_{ij}(x)dv \quad (3)$$

Furthermore, Hooke's generalized law is:

$$\sum_{ij} = C_{ijkl}E_{kl} \quad (4)$$

The law of mixtures applied to the composite gives [2,4] :

$$E_{ij} = \frac{V^r}{V}\varepsilon_{ij}^r + \frac{V^m}{V}\varepsilon_{ij}^m \quad (5.1)$$

$$\sum_{ij} = \frac{V^r}{v}\sigma_{ij}^r + \frac{V^m}{V}\sigma_{ij}^m \quad (5.2)$$

By positing $f = f^r = \frac{V^r}{V}$, from equations (3), (4) and (5) we show that:

$$C_{ijkl} = C_{ijkl}^m + f(C_{ijkl}^r - C_{ijkl}^m)A_{klmn}^r \quad (6.1)$$

According to Voigt's hypothesis,

$A_{klmn}^r = I_{ijkl}$ (identity tensor)

So we have :

$$C_{ijkl} = C_{ijkl}^m + f(C_{ijkl}^r - C_{ijkl}^m) \quad (6.2)$$

When the film is subjected to unidirectional tensile stress, equation (6.2) becomes:

$$E = E^m + f(E^r - E^m) \quad (7)$$

From (1) and (7), we finally derive the law of homogenized thermomechanical behavior:

$$E = \frac{(1-f)E_o^m R_e^r\left(R_e^m - C_s E_o^m \alpha_{th}^m \Delta T\right) + f E_o^r R_e^m\left(R_e^r - C_s E_o^r \alpha_{th}^r \Delta T\right)}{R_e^m R_e^r} \quad (8)$$

The next step will focus on the calculation by simulation of the displacement at the crack tip using the law established in equation (8).

The next step will focus on the calculation by simulation of the displacement at the crack tip using the law established in equation (8).

4. SIMULATION OF FRACTURE BEHAVIOR: EFFECTS OF TEMPERATURE AND REINFORCEMENT

4.1 Methods, Mesh and Boundary Conditions

The simulation is done using the Cast3M finite element calculation code. We will adopt the Extended Finite Elements method (XFEM) and we will remain within the framework of plane deformations. The sample film contains an artificial square-shaped crack of side w (in mm), of length L (in mm), centered and inclined at an angle β relative to the axis orthogonal to the direction of the stress. This is a uniform unidirectional traction following the horizontal. For the mesh, the finite element chosen is the quadrangle with eight nodes (QUA8) which is

more representative of the geometry and boundary conditions. The density at the crack tip is twenty times higher than that of the elements at the periphery of the sample (Fig. 2).

The data used are shown in Table 1.

4.2 Simulation Results

The results are presented to illustrate the effects of variations in reinforcement and temperature on the behavior of the composite film with respect to crack propagation. This allows us to better understand its resistance to rupture.

The results obtained are shown in Tables 2 to 5. The different cases are represented by a three-part code as illustrated by the two examples in the appendix.

4.2.1 Crack tip displacements as a function of temperature

In both cases, we observe that the crack displacement increases in absolute value as the temperature increases. This is corroborated by Fig. 3. which present the deformations of the film at different temperature variations for f=0.03 and r=0.15mm and σ_A=3.2 MPa fixed. They illustrate the behavior of the composite at (local) failure.

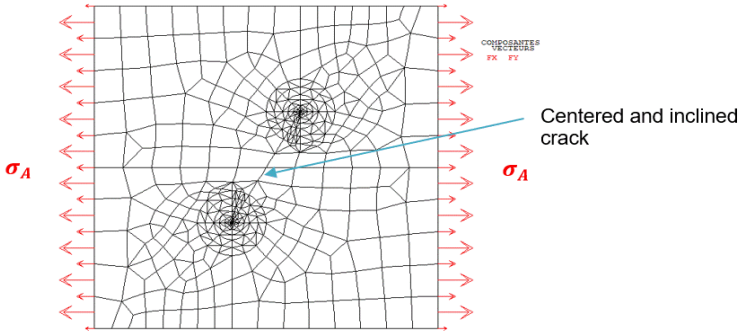

Fig. 2. Mesh of the cracked film sample and boundary conditions

Table 1. Geometric, mechanical and thermal properties of the cracked film sample

	β	σ_A	L	W	E	E_o^m	E_o^r	R_e^m	R_e^r	C_s	α_{th}^m	α_{th}^r
Valeurs	30	3.2	50	250	Eq . 8	37	4500	2.1	175	0,66	137.10^{-6}	$4.7.10^{-6}$

Table 2. Crack tip displacements as a function of temperature at different fiber volume fractions for r = 0.6mm

T	0	5	10	15	20	25	30	35	40	45
1vr06f003	212.81	213.23	213.66	214.09	214.51	214.94	215.38	215.81	216.25	216.69
1vr06f0015	349.86	350.93	352.015	353.09	354.19	355.28	356.39	357.50	358.62	359.74
1vr06f006	119.32	119.47	119.62	119.78	119.93	120.08	120.23	120.39	120.54	120.69
1ur06f003	-238.84	-239.32	-239.79	-240.27	-240.75	-241.24	-241.72	-242.21	-242.70	-243.19
1ur06f0015	-392.66	-393.87	-395.07	-396.29	-397.52	-398.75	-399.99	-401.24	-402.49	-403.75
1ur06f006	-133.92	-134.09	-134.26	-134.43	-134.6	-134.77	-134.94	-135.11	-135.28	-135.46

Table 3. Crack tip displacements as a function of temperature at different fiber volume fractions for r = 0.15 mm

T	0	5	10	15	20	25	30	35	40	45
vr015f003	11.086	11.088	11.09	11.092	11.095	11.097	11.099	11.102	11.104	11.106
vr015f0015	174.93	175.47	176.01	176.55	177.09	177.64	178.2	178.75	179.31	179.87
vr015f006	59.661	59.736	59.812	59.888	59.964	60.04	60.116	60.193	60.269	60.34
ur015f003	-119.42	-119.66	-119.9	-120.14	-120.38	-120.62	-120.86	-121.11	-121.35	-121.6
Ur015f0015	-196.33	-196.93	-197.54	-198.15	-198.76	-199.37	-199.99	-200.62	-201.25	-201.88
ur015f006	-66.959	-67.043	-67.128	-67.213	-67.299	-67.384	-67.47	-67.556	-67.642	-67.72

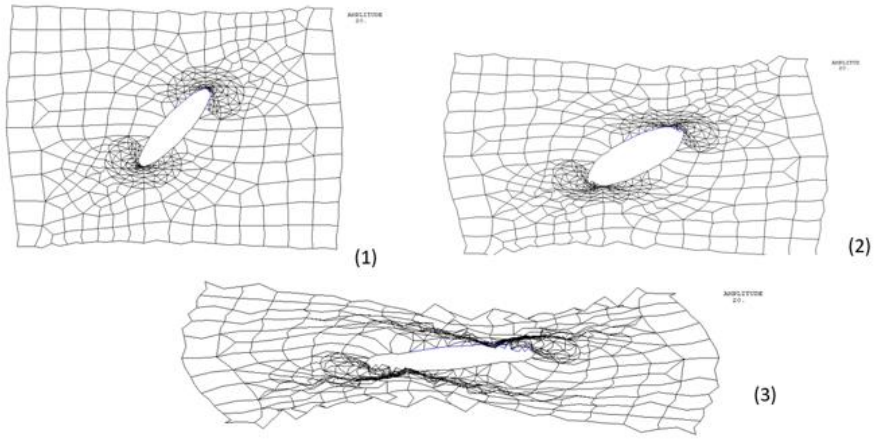

Fig. 3. Deformation of the composite film as a function of temperature variation: (1) ∆T=5oC, (2) ∆T=20oC, (3)) ∆T=40oC à f=0,03 et r=0,15mm

4.2.2 Crack tip displacements as a function of fiber volume fraction

In both cases, we find that the crack tip displacement decreases in absolute value as the volume fraction of fibers in the composite increases. This phenomenon can be observed in Fig 4, which show the deformations of the film at different volume fractions of fibers; for ∆T= 10oC, r=0.15mm and σA=3.2 MPa fixed. They illustrate the behavior of the composite at (local) failure.

Table 4. Crack tip displacements as a function of the volume fraction of the fibers at different temperature variations for r = 0.60 mm

f	0.1	0.2	0.3	0.4	0.5	0.6	0.7	0.8	0.9
1vr06T5	75.3162	39.146	26.4456	19.9674	16.0386	13.4017	11.5094	10.0853	8,97491
1vr06T10	448.91	289.52	213.66	169.3	140.19	119.62	104.32	92.487	83.065
1vr06T30	75.6646	39.2717	26.5174	20.0166	16.0756	13.4312	11.5339	10.1063	8.99316
1ur06T5	-84.5293	-43.9345	-29.6806	-22.41	-18.0005	-15.041	-12.9173	-11.319	-10.0728
1ur06T10	-503.83	-324.94	-239.79	-190.01	-157.34	-134.26	-117.08	-103.8	-93.226
1ur06T30	-84.9203	-44.0756	-29.7612	-22.4652	-18.0421	-15.0742	-12.9448	-11.3426	-10.0932

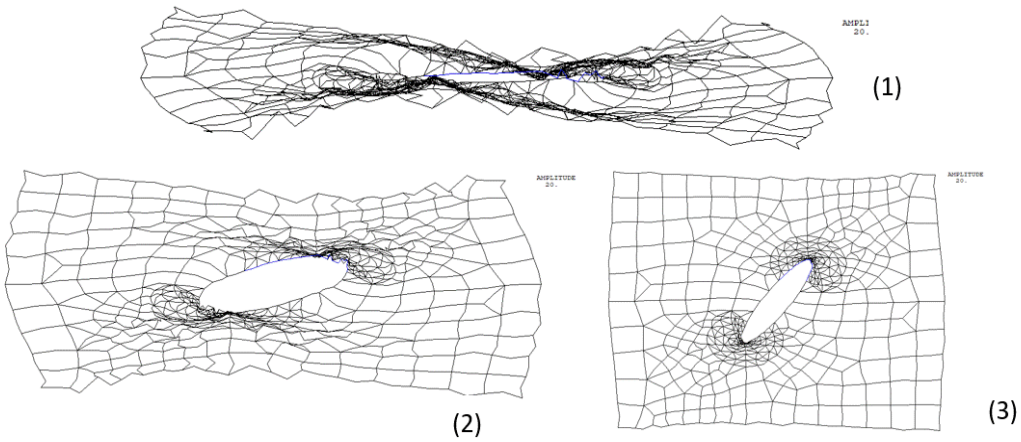

Fig. 4. Deformation of the composite film as a function of the variation in the volume fraction of the fibers : (1) f=0.01, (2) f=0.04, (3)f=0.08

Table 5. Crack tip displacements as a function of the volume fraction of the fibers at different temperature variations for r = 0.15 mm

f	0.1	0.2	0.3	0.4	0.5	0.6	0.7	0.8	0.9
1vr015T5	45.32	23.7462	16.0878	12.1646	9.77975	8.17669	7.02516	6.15793	5.48129
1vr015T10	224.46	144.76	106.83	84.649	70.095	59.812	52.16	46.243	41.533
1vr015T30	37.8323	19.6358	13.2587	10.0083	8.03782	6.71561	5.76696	5.05315	4,49658
1ur015T5	-42.2646	-21.9673	-14.8403	-11.205	-9.00027	-7.52051	-6.45863	-5.65952	-5.03638
1ur015T10	-251.91	-162.47	-119.9	-95.003	-78.67	-67.128	-58.54	-51.9	-46.613
1ur015T30	-42.4602	-22.0378	-14.8806	-11.2326	-9.02105	-7.5371	-6.47241	-5.67128	-5.04662

5. HOMOGENIZED ASYMPTOTIC DISPLACEMENT FIELDS IN MIXED RUPTURE MODE

Fig 5. represents the local reference in the vicinity of the crack front. (r, β) are the coordinates of a point very close to the crack front in a cylindrical coordinate system centered on the crack tip. Let M be a point with coordinates (x, y) in the plane (O, x, y), we have x = r cosβ and y = r sinβ.

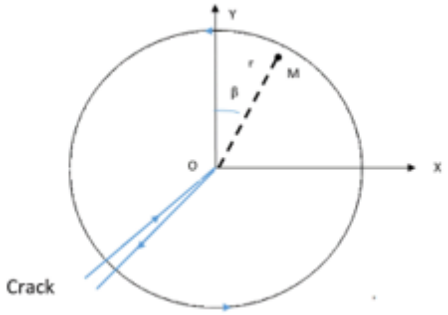

Fig. 5. Setting the crack tip

Westergaard's approach [3] makes it possible to obtain, using Airy functions, the movements in the vicinity of the front, except that here there is a permutation of the roles of the axes:

$$\begin{cases} u = \frac{1}{2\mu}\sqrt{\frac{r}{2\pi}}\left[K_I \sin(\frac{\beta}{2})(k - \cos(\beta) + K_{II}\cos\left(\frac{\beta}{2}\right)(k - 2 + \cos(\beta))\right] \\ v = \frac{1}{2\mu}\sqrt{\frac{r}{2\pi}}\left[K_I \cos(\frac{\beta}{2})(k - \cos(\beta) + K_{II}\sin\left(\frac{\beta}{2}\right)(k + 2 + \cos(\beta))\right] \end{cases} \quad (9)$$

where :

$$k=3-4\nu \quad (10.1)$$

$$\mu = \frac{E}{2(1+\nu)} \quad (10.2)$$

And :

$$K_I = \sigma_A\sqrt{\pi L}\,(\cos\theta)^2 \quad (11.1)$$

$$K_{II} = \sigma_A\sqrt{\pi L}\cos\theta\sin\theta \quad (11.2)$$

From equations (8) and (10), we have :

$$\mu = \frac{(1-f)E_o^m R_e^r\left(R_e^m - C_s E_o^m \alpha_{th}^m \Delta T\right) + f E_o^r R_e^m\left(R_e^r - C_s E_o^r \alpha_{th}^r \Delta T\right)}{2(1+\nu)R_e^m R_e^r} \quad (12)$$

Finally, from relations (9), (11) and 12, we obtain the analytical expressions of the asymptotic fields of the homogenized displacements in the vicinity of the crack tip :

$$\begin{cases} u = \dfrac{(1+\nu)R_e^m R_e^r\sqrt{\frac{r}{2\pi}}\left[K_I \sin(\frac{\beta}{2})(k - \cos(\beta) + K_{II}\cos\left(\frac{\beta}{2}\right)(k - 2 + \cos(\beta))\right]}{(1-f)E_o^m R_e^r(R_e^m - C_s E_o^m \alpha_{th}^m \Delta T) + f E_o^r R_e^m(R_e^r - C_s E_o^r \alpha_{th}^r \Delta T)} & (13.1) \\ v = \dfrac{(1+\nu)R_e^m R_e^r\sqrt{\frac{r}{2\pi}}\left[K_I \cos(\frac{\beta}{2})(k - \cos(\beta) + K_{II}\sin\left(\frac{\beta}{2}\right)(k + 2 + \cos(\beta))\right]}{(1-f)E_o^m R_e^r(R_e^m - C_s E_o^m \alpha_{th}^m \Delta T) + f E_o^r R_e^m(R_e^r - C_s E_o^r \alpha_{th}^r \Delta T)} & (13.2) \end{cases}$$

6. COMPARATIVE ANALYSIS AND DISCUSSION

In this part, we will make a comparison of the results from equation (12)(analytical) and those obtained by simulation in the Cast3M software. For the simulation, we used the experimental data and took into account the hypotheses of the study (Cf 2.). The movements are recorded and reported in MatLab for plotting the different graphs. A comparison is made in order to judge their agreement. The two series of curves (analytical and Cast3M) are given in Fig. 6 and 7. The nomenclature of the legends is given in the appendix.

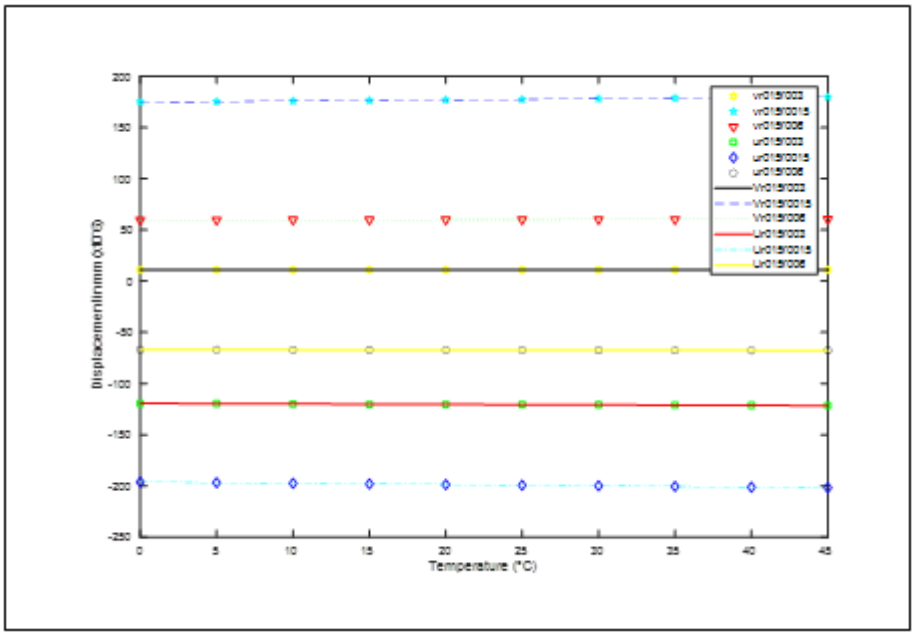

(Fig. 6.a)

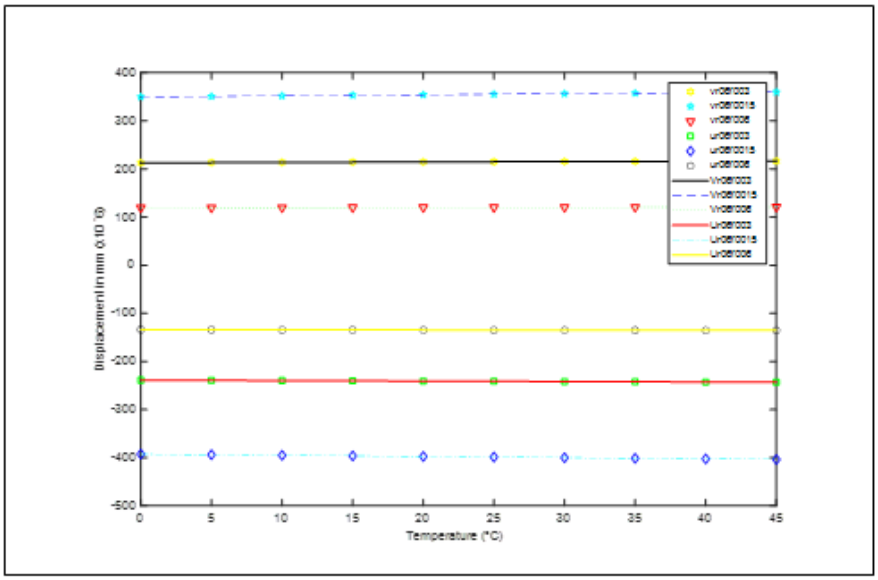

(Fig. 6.b)

Fig. 6. Evolution of the displacement at the crack tip as a function of the temperature at different volume fractions of the fibers for (1) r = 0.15 mm et (2) r=0.6 mm

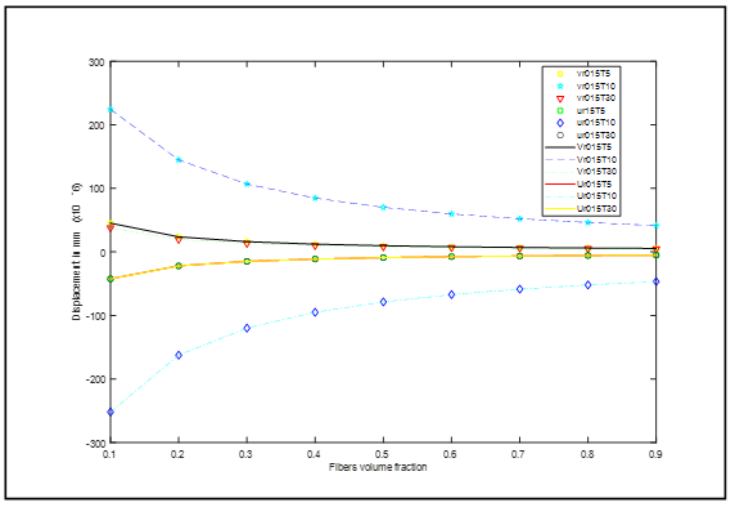

(Fig. 7.a)

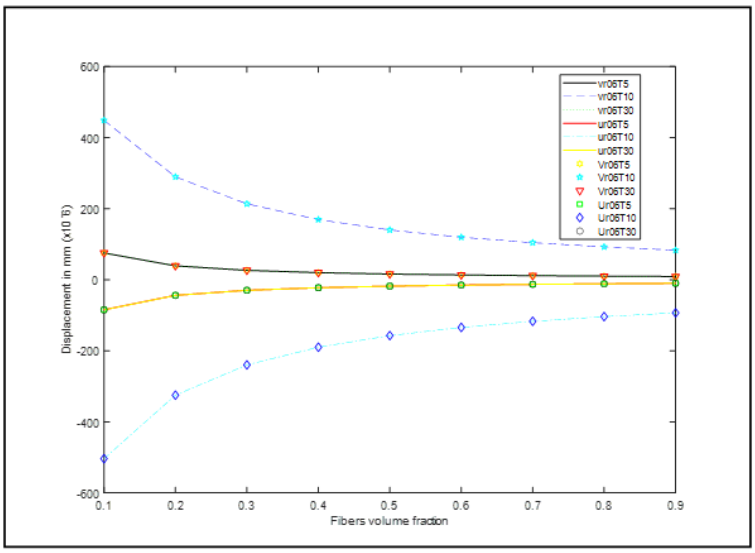

(Fig. 7.b)

Fig. 7. Evolution of the displacement at the crack tip as a function of the volume fraction of the fibers at different temperature variations for (1) r = 0.15 mm et (2) r=0.6 mm

We note that in all cases, the two series of curves resulting respectively from the analytical values and the simulation under Cast3M are perfectly superimposable.

When the temperature variation increases from 0 to 45 ^{o}C, (Fig. 6), the displacements have a slight increase in absolute values. The crack tip has a reduced displacement. However, this does not prevent the remarkable fracture states for low fiber ratios (Fig. 3). Temperature is a destructive factor in the structure of this composite [2, 4]. We can for example notice that at r=0.6mm and f=0.03, the crack tip moves from -238.84.10^{-6} mm to -243.191.10^{-6} mm horizontally and from 212.808.10^{-6} mm to - 216,685.10^{-6} mm vertically (Cast3M values).

We also note that with the increase in the volume fraction of fibers, the displacements of the crack tip undergo a rapid decrease (Fig. 7). For example, for r=0.15mm and T=10^{o}C, the horizontal and vertical displacements go from 22.446.10^{-5} and -25.191.10^{-5} mm to 4.1533.10^{-5} and -4.6613.10^{-5} respectively (Cast3M values) . They allow the composite to have a more

resistant behavior to breakage. Indeed, the presence of fibers increases the rigidity of the material [2, 4] with the creation of bridges between the polymer chains. (Fig. 4).

In all cases, the horizontal displacement always remains greater in absolute value than the vertical displacement. This is due to the angular position of the crack, $\beta=30^{o}$ relative to the vertical axis. In this geometric configuration, the loading gives predominance to mode I in the horizontal direction. It is this mode which is more critical in a mixed situation of rupture as is the case in the present study.

7. CONCLUSION

The objective of this work was to analyze the effects of temperature and fibers on the breaking behavior of a composite based on cassava starch reinforced with coconut fibers. To do this, we adapted two approaches based on the calculation of the displacement of the crack tip using the extended finite element method (XFEM). The first consisted of a simulation taking into account an established homogenized thermomechanical behavior law. The second is an analytical study based on homogenized asymptotic solutions of the fracture in displacement of the crack tip. A comparison showed a very high agreement between the two approaches. We thus obtain a model for the analysis of the breaking behavior, as a function of temperature and fiber content, of this composite film.

COMPETING INTERESTS

Authors have declared that no competing interests exist.

REFERENCES

1. Ahmed Doumbia, Pierre R. Dable, Edja F. Assanvo, Development and characterization of a biodegradable material based on cassava starch reinforced by coconut mesocarp microfibers; Afrique Science. 2018;14(5): 400 – 414
2. Ahmed Doumbia, Pierre JMR. Dable. Analysis of the Thermo-Mechanical Behavior of composite materials based on plasticized cassava starch reinforced with coconut fibers; Indian Journal of Science and Technology. 2019;12(4). DOI: 10.17485/ijst/2018/v12i4/140015
3. BUI H. Mechanics of brittle fracture. Masson, Paris, 1st edition; 1978.
4. Doumbia Ahmed, Unique doctoral thesis; Development of Composite Materials Based on Cassava Starch Reinforced by Coconut Mesocarp Fibers: Study of Physicochemical Stability, Mechanical and Thermomechanical Behavior and Applicability to Packaging; INP-HB; 2020.
5. Jean-François G. Tensors, variations and continuous media, Local and variational formulations of the mechanics of elastic continuous media, Technosup. Paris ; 2003;184-211,
6. Voigt W, Wied Ann Mech. 1889 ;38:573-587.
7. Durif E, Réthoré J, Combescure A, Development of an enriched Finite Element method adapted to the modeling of multifissured structures, NSA / LAMCOS, UMR/CNRS 5559 Bât. J. d'Alembert, 20 avenue Albert Einstein, 69621 Villeurbanne Cedex

APPENDIX

Examples of nomenclature of the different cases analyzed:

Example 1: for analyzing the effect of temperature variation
Ur06f003: u(horizontal displacement), r06(at a distance of 0.6mm from the crack tip), f003(with a fiber volume fraction equal to 0.03),
Vr06f003: v(vertical displacement), r0.6(at a distance of 0.6mm from the crack tip), f003(with a fiber volume fraction equal to 0.03).

Example 2: for analyzing the effect of varying the volume fraction of fibers
Ur06t10: u(horizontal displacement), r06(at a distance of 0.6mm from the crack tip), t10(with a temperature variation equal to 10^{o}C),
Vr06t10: v(vertical displacement), r06(at a distance of 0.6mm from the crack tip), t10(with a temperature variation equal to 10^{o}C).

Peer-review history:
The peer review history for this paper can be accessed here:
https://www.sdiarticle5.com/review-history/111693